Rock and Soil Mechanics

Volume 43 | Issue 4 Article 3

6-9-2022

Experimental study of sandstone crack propagation behavior under different seepage pressures

Li-ming ZHANG
Cooperative Innovation Center of Engineering Construction and Safety in Shandong Blue Economic Zone, Qingdao University of Technology, Qingdao, Shandong 266033, China

Zai-quan WANG
Cooperative Innovation Center of Engineering Construction and Safety in Shandong Blue Economic Zone, Qingdao University of Technology, Qingdao, Shandong 266033, China, zqwang4521@163.com

Tian-yang ZHAO
School of Science, Qingdao University of Technology, Qingdao, Shandong 266033, China

Yu CONG
Cooperative Innovation Center of Engineering Construction and Safety in Shandong Blue Economic Zone, Qingdao University of Technology, Qingdao, Shandong 266033, China

Custom Citation

ZHANG Li-ming, WANG Zai-quan, ZHAO Tian-yang, CONG Yu, . Experimental study of sandstone crack propagation behavior under different seepage pressures[J]. Rock and Soil Mechanics, 2022, 43(4): 901-908.

Rock and Soil Mechanics 2022 43(4): 901−908 ISSN 1000−7598
https: //doi.org/10.16285/j.rsm.2021.5667 rocksoilmech.researchcommons.org/journal

Experimental study of sandstone crack propagation behavior under different seepage pressures

ZHANG Li-ming[1, 2], WANG Zai-quan[1, 2], ZHAO Tian-yang[3], CONG Yu[1, 2]

1. School of Civil Engineering, Qingdao University of Technology, Qingdao, Shandong 266033, China
2. Cooperative Innovation Center of Engineering Construction and Safety in Shandong Blue Economic Zone, Qingdao University of Technology, Qingdao, Shandong 266033, China
3. School of Science, Qingdao University of Technology, Qingdao, Shandong 266033, China

Abstract: To study the characteristics of sandstone crack propagation under hydraulic coupling, sandstone laboratory tests were conducted under different seepage pressures and confining pressures. Under the same effective confining pressure, it is shown that the rock brittleness index becomes higher as the seepage pressure increases, while the crack initiation stress, the crack damage stress, and the peak stress decrease gradually. The initial volumetric strain of the crack decreases, and the volumetric strain of crack propagation decreases firstly and then increases afterward. The growth rate of the crack axial strain and the crack circumferential strain are both increasing that corresponding to the damage stress and the peak stress, however, no obvious relation is observed between the growth rate of the crack volume strain and the seepage pressure. Under the same seepage pressure, the initiation stress, damage stress, and peak stress gradually increase as the effective confining pressure increases. In addition, the growth rates of the crack axial strain, circumferential strain and volumetric strain increase gradually during deformation that corresponds to the crack initiation stress, damage stress and peak stress, respectively. When comparing the different growth rates of crack strain for a tested sandstone specimen, it is found that the strain growth rates have the following order: the crack axial strain > the crack circumferential strain > the crack volume strain.

Keywords: hydraulic coupling; characteristic stress level; crack growth rate

1 Introduction

For the rock engineering projects such as underground caverns, underground mining excavation and diversion tunnels, the rock masses are directly affected by the groundwater, which usually causes water inrush accidents and seriously affects the project safety. The physical/mechanical properties, characteristics of the failure behavior and crack evolution of rock masses are significantly different with and without water conditions[1−2]. It is therefore important to study the progressive failure process, mechanical characteristics, and deformation laws of rock masses under hydro-mechanical coupling effect.

For the mechanical characteristics of rocks under hydro-mechanical coupling, researchers are mainly focused on the relations between permeability and confining pressure, axial pressure and deformation. Yu et al.[3] supposed that the volume strain variation of the sandstone is directly related to the permeability evolution process. Zhao et al.[4] carried out permeability tests on fractured specimens and obtained the variation law of permeability with the confining pressure for different joint surfaces. Based on the permeability test of sandstone, Peng et al.[5] found that the permeability was closely related to the magnitude of the effective confining pressure. Hu et al.[6] supposed a correspondence relationship between the effective stress coefficient and axial deformation. Park[7] studied the permeability of sedimentary rocks, and found that the permeability increased as the axial stress increased. For sandstone, Li et al.[8] found there is a close relationship between the permeability and the axial stress/strain.

For the progressive failure and crack propagation of rocks under hydro-mechanical coupling, Bieniawski[9] and Martin[10] believed that the progressive failure process of rocks is directly related to the crack closure, crack initiation and expansion. Wang et al.[11] analyzed the relation between the crack strain and permeability of gneisses at various stages, and they concluded that there is a correspondence between the development trend of crack circumferential strain and permeability evolution characteristics. Zhou et al.[12] concluded that

Received: 3 May 2021 Revised: 13 November 2021
This wok was supported by the Natural Science Foundation in Shandong Province (ZR2020ME099, ZR2020MD111) and the National Natural Science Foundation of China (52179104).
First author: ZHANG Li-ming, male, born in 1977, PhD, Professor, mainly engaged in research on rock mechanics and underground engineering. E-mail: dryad_274@163.com
Corresponding author: WANG Zai-quan, male, born in 1964, PhD, Professor, engaged in teaching and scientific research in geotechnical engineering. E-mail: zqwang4521@163.com

the seepage pressure and axial stress exacerbate the propagation of branching cracks. Cao et al.[13] analyzed the mechanism of crack initiation and penetration within the rock specimens, and they found that the hydraulic pressure had an inhibitory effect on the petal-shaped cracks and anti-flanking cracks. Wang et al.[14] used the extended finite element method (XFEM) to simulate the 3D crack propagation process under hydro-mechanical coupling and they found that the crack propagation direction was parallel to the vertical stress under the Darcy's seepage condition.

The evolution of rock permeability characteristics has been widely studied, while the analysis of rock crack propagation behavior was focused on the regular macroscopic failure characteristics and crack strain law, lacking study on the rock crack growth rate under hydraulic pressure. This study mainly focuses on the relation between sandstone crack strain and seepage pressures under the effect of conventional Tri-axial and hydro-mechanical coupling. The evolutionary characteristics of axial crack growth rate, circumferential crack growth rate and volumetric crack growth rate during the loading process are also explored.

2 Introduction of the experiment

2.1 Specimens preparation

The sandstone block samples were collected from the field, and cylindrical specimens were obtained by drilling and coring with a drilling rig. Standard cylindrical specimens (with a diameter of 50 mm and a height of 100 mm) were then prepared through the secondary processing in the laboratory, which meets the standard requirements of the "*Standard for test methods of engineering rock mass*"[15]. The specimens were selected for the laboratory tests with wave velocities between 2 900 m/s and 3 000 m/s.

2.2 Test instrument and schemes

The tests were conducted using the rock triaxial stress−seepage coupling test system, as shown in Fig.1. The procedure of the hydro-mechanical coupling test is as follows: the sandstone was vacuum-saturated for 24 h, and the confining pressure is applied to 7, 10, and 15 MPa at a loading rate of 0.25 MPa/s. The water pressure at the outlet position was equal to the atmospheric pressure of 0.1 MPa, and the pressure at the inlet position was 1.1, 3.1, and 5.1 MPa until a uniform water flow was observed at the outlet location, and the differential seepage pressure was 1.0, 3.0, and 5.0 MPa, respectively. Afterwards, the axial force was loaded at an increasing rate of 0.04 mm/min until the rock specimen reached a failure state.

Fig. 1 Rock triaxial stress−seepage coupling test system

3 Analysis of the experiment results

3.1 Failure characteristics

Table1 shows the photos of the failed sandstone specimens, where the fracture surface shows obvious shear failure characteristics. Under the conventional triaxial test condition, the fracture surface traces of the failure specimens are clearly visible, and the upper and lower shear surfaces are obviously dislocated. The two sides of the fracture surface can be separated easily by hand. While under the seepage pressure loading condition, the traces of sandstone failure are blurred, and it is difficult to separate the two sides of the fracture surface by hand.

Table 1 Macroscopic failure characteristics of sandstone under different loading paths

Confining pressure /MPa	Failure characteristics under different seepage pressures (MPa)			
	0	1	3	5
7				
10				
15				

Hu et al. [6] proposed a brittleness index B_1 based on the rock deformation stress−strain curve:

$$B_1 = \frac{\sigma_f - \sigma_t}{\sigma_f} \quad (1)$$

where σ_f is the peak stress; σ_t the residual stress.

The brittleness index B_1 considers the magnitude of the post-peak stress drop, and the larger the stress drop, the more brittle it is. The brittleness indexes of sandstone failure under different stress paths are shown in Table 2.

Table 2 Brittleness index B_1 of sandstone

Confining pressure /MPa	Seepage pressure /MPa	Effective confining pressure /MPa	Brittleness index B_1
7	0	7	0.200
	1	6	0.210
	3	4	0.460
	5	3	0.360
10	0	10	0.120
	1	9	0.170
	3	7	0.210
	5	5	0.310
15	0	15	0.040
	1	14	0.052
	3	12	0.024
	5	10	0.026

The confining pressure on the rock skeleton under seepage pressure is expressed as effective confining pressure:

$$P_f = \sigma_3 - \Delta P \quad (2)$$

where P_f is the effective confining pressure; σ_3 is the confining pressure; and ΔP is seepage pressure.

As the seepage pressure increases, the effective confining pressure decreases, and the brittleness index of the rock specimens increases. This observation can be explained based on the Biot effective stress principle[1]. Under the same confining pressure, the effective confining pressure decreases as the seepage pressure increases, which weakens the inhibition effect of the effective confining pressure on the internal crack. Thus, the internal microcracks and the pores are therefore easy to expand and open, and the rock brittleness becomes stronger and the brittleness index increases then. When the confining pressure is 7 MPa, the rock brittleness index under 3 MPa seepage pressure is higher than that under 5 MPa seepage pressure, which may be caused by the heterogeneity of the rock specimens. In addition, the brittleness index with 15 MPa confining pressure is found to be one order of magnitude less than those with the confining pressures of 7 MPa and 10 MPa. It can be explained that the higher confinement (15 MPa) increases the effective confining pressure, and the inhibition of internal microcracks and pores is enhanced, resulting in a smaller brittleness index.

3.2 Characteristics of the stress−strain curve

Figure 2 shows the stress−strain curves of the sandstone under the conventional triaxial test. Figure 3 shows the stress-strain curves of the sandstone with different seepage pressures under the same confinements. Figure 4 shows the stress−strain curves of the sandstone under different confining pressures with the same seepage pressures. Each test curve is labelled as a form of Letter−Number 1−Number 2, where the letter indicates the test type: UC means the uniaxial compressive test, CS means the triaxial compressive test, and RS means the seepage-stress coupling test; number 1 indicates the confining pressure, and number 2 indicates the seepage pressure, D indicates dry, and S indicates saturation. Table 3 shows the strains associated with the peak stress of sandstone under different stress loading paths.

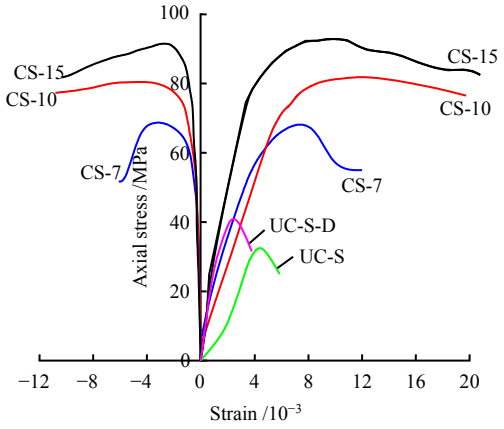

Fig. 2 Stress−strain curves of sandstone samples under conventional triaxial test

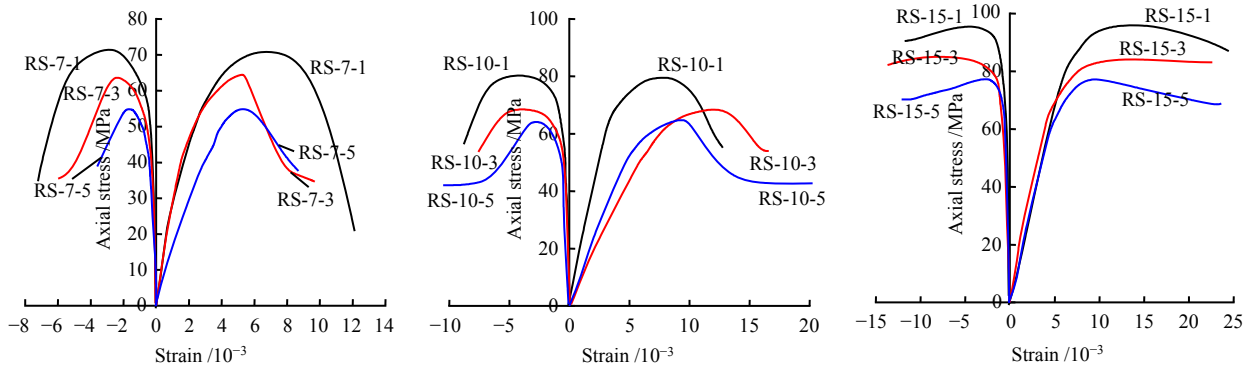

(a) Confinement stress: 7 MPa (b) Confinement stress:10 MPa (c) Confinement stress:15 MPa

Fig. 3 Stress−strain curves of sandstone samples under different seepage pressures with three confinements

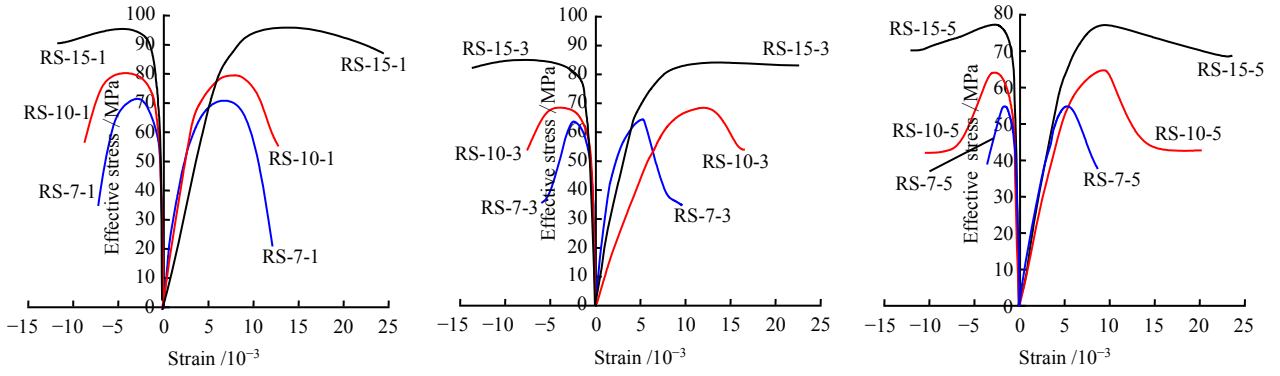

(a) Seepage pressure 1 MPa (b) Seepage pressure 3 MPa (c) Seepage pressure5 MPa

Fig. 4 Stress−strain curves of sandstone samples under different confining pressures with three seepage pressures

Table 3 The strains associated with the peak strength of sandstone under different stress loading paths

Specimen No.	Effective confining pressure /MPa	Peak axial strain /10^{-3}	Peak circumferential strain /10^{-3}
UC-D	—	1.9	—
UC-S	—	6.9	—
CS-7	7	6.8	−2.5
CS-10	10	11.1	−4.6
CS-15	15	8.5	−2.1
RS-7-1	6	7.1	−3.1
RS-7-3	4	5.5	−2.4
RS-7-5	3	5.7	−1.8
RS-10-1	9	8.0	−4.5
RS-10-3	7	12.0	−4.5
RS-10-5	5	9.3	−2.4
RS-15-1	14	12.1	−4.8
RS-15-3	12	12.0	−8.4
RS-15-5	10	9.8	−2.5

It is found that the stress-strain curve of the UCS test falls rapidly after reaching the peak stress. The peak stress is 41.2 MPa for the dry sandstone, and 33.5 MPa for the saturated sandstone. The axial strain is 1.9×10^{-3} corresponding to the peak stress of the dry sandstone, which is smaller than that of the saturated sandstone (4×10^{-3}). Under the same confining pressure, as the seepage pressure increases, the effective confining pressure, the peak stress, as well as the circumferential strain corresponding to the peak stress decreases. Compared with the test results of the conventional triaxial tests, the peak stress of sandstone significantly decreases when the seepage pressures are 3 MPa and 5 MPa. When the seepage pressure is 1 MPa, the variation of peak stress is not obvious compared with the conventional triaxial. Under low confinement, it is found that the low seepage pressure has a limited effect on the strength of specimens, which is in agreement with the results of Yu et al.[3].

3.3 Analysis of crack propagation process

The volume strain can be decomposed into two parts[10, 16−17]: one part is the crack volume strain $\varepsilon_{\mathrm{v}}^{\mathrm{c}}$, which is caused by the crack closure, new crack initiation and coalescence within the rock during loading; the other part is the elastic volume strain $\varepsilon_{\mathrm{v}}^{\mathrm{e}}$ at the same stress level. Similarly, the crack axial strain $\varepsilon_1^{\mathrm{c}}$ and crack circumferential strain $\varepsilon_3^{\mathrm{c}}$ are then obtained by the axial strain ε_1 and circumferential strain ε_3 subtract the corresponding elastic strains in the same direction:

$$\varepsilon_{\mathrm{v}} = \varepsilon_1 + 2\varepsilon_3 \tag{3}$$

$$\varepsilon_{\mathrm{v}}^{\mathrm{c}} = \varepsilon_{\mathrm{v}} - \frac{1-2\mu}{E}\left(\sigma_1 + 2\sigma_3\right) \tag{4}$$

$$\varepsilon_1^{\mathrm{c}} = \varepsilon_1 - \frac{\sigma_1 - 2\mu\sigma_3}{E} \tag{5}$$

$$\varepsilon_3^{\mathrm{c}} = \varepsilon_3 - \frac{\sigma_3 - \mu\left(\sigma_1 + \sigma_3\right)}{E} \tag{6}$$

where ε_1, ε_3, and ε_{v} are the axial strain, circumferential strain and volume strain of the rock specimens, respectively; $\varepsilon_1^{\mathrm{c}}$, $\varepsilon_3^{\mathrm{c}}$, and $\varepsilon_{\mathrm{v}}^{\mathrm{c}}$ are the crack axial strain, crack circumferential strain and crack volume strain, respectively; μ is the Poisson's ratio; E is the modulus of elasticity; σ_1 and σ_3 are the axial stress and confining pressure, respectively.

The characteristic stresses of the sandstone are calculated using the crack-strain model proposed by Martin[10]. The sandstone stress−strain curve is divided into five stages, as shown in Fig.5. Stage I is the crack compression closure stage, and the end of this stage corresponds to the crack closure stress. Stage II is the elastic deformation stage, and the end of this stage corresponds to the crack initiation stress. Stage III is the crack stable propagation stage, which ends at the damage stress, after which the rock volume changes from compression to expansion. Stage IV is the crack unstable propagation stage, and the volume expansion of the rock sample accelerates. After the peak stress, the sandstone enters the strain-softening stage V.

Figure 5 shows the relation curves among the volume strain, crack volume strain and axial strain under different stress loading paths. The initial crack volume strain is the crack volume strain corresponding to the initiation stress, and the crack extension volume strain is the crack volume strain corresponding to the peak stress. Table 4 is the statistical results of the characteristic stress of sandstone under different loading paths.

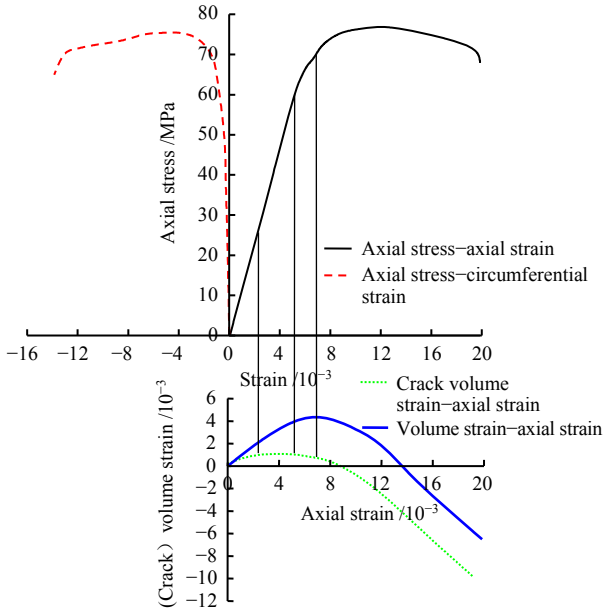

(a) Conventional triaxial confining pressure 10 MPa

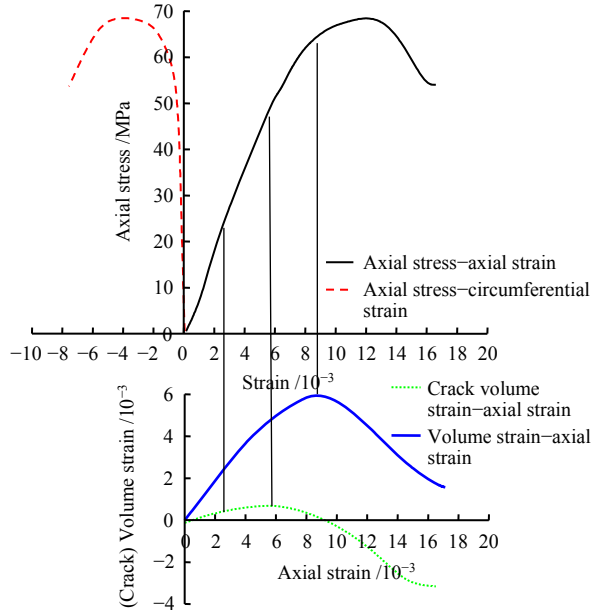

(b) Confining pressure 10 MPa, seepage pressure3 MPa

Fig. 5 The relations among the volume strain, crack volume strain and axial strain under different stress loading paths

Table 4 Statistical results of characteristic stress levels of sandstone under conventional triaxial and hydro-mechanical coupling tests

Specimen No.	Initiation stress σ_{ci} /MPa	Damage stress σ_{cd} /MPa	Peak stress σ_f /MPa	Initiation stress ratio σ_{ci}/σ_f	Damage stress ratio σ_{cd}/σ_f
CS-7	46.5	55.0	70.0	0.751	0.887
CS-10	59.1	70.1	82.6	0.756	0.893
CS-15	72.3	85.3	94.3	0.769	0.907
RS-7-1	46.8	61.1	72.3	0.634	0.847
RS-7-3	42.3	52.8	65.8	0.647	0.808
RS-7-5	35.6	52.0	56.1	0.630	0.920
RS-10-1	61.9	72.0	81.2	0.773	0.900
RS-10-3	49.5	65.2	70.2	0.702	0.922
RS-10-5	51.4	60.2	65.2	0.791	0.923
RS-15-1	69.5	89.3	96.0	0.732	0.930
RS-15-3	60.5	80.7	86.5	0.712	0.932
RS-15-5	58.0	72.9	77.6	0.743	0.939

Under the same confining pressure, the effective confining pressure decreases as the seepage pressure increases, and the damage stress and peak stress also decrease. Under the confinement of 10 MPa and the seepage pressure of 3 MPa, the value of crack initiation stress is relatively small, which may be caused by the heterogeneity of the specimen. Under the same seepage pressure, the crack initiation stress and damage stress increase as the effective confining pressure increases. Under conventional triaxial conditions, the ratio between crack initiation stress and peak stress ranges from 0.75 to 0.77, which agrees with the results of Martin[10] where the ratios of fine-grained siltstone and limestone to sandstone are 0.6 to 0.8. The ratio between damage stress and peak stress ranges from 0.85 to 0.91, which is higher than the results (0.70 to 0.85) of Bieniawski[9]. Under the acting of seepage pressure, the ratio of crack initiation stress and peak stress is between 0.63 and 0.79, and the ratio of damage stress to peak stress is between 0.81 and 0.94. The presence of seepage pressure leads to significant drops in peak stress, which cause a higher ratio of damage stress to peak stress. The damage stress is closer to the peak stress, which indicates that the specimen's internal cracks instantly develop in all directions rapidly after the stress exceeds the damage stress.

Figure 6 shows the relations between the initial volume strain of crack ε_v^{co}, the volume strain of crack propagation ε_v^{cp} and the seepage pressure under different confining pressures. Under the same confining pressure, the initial volume strain of the crack decreases as the seepage pressure increases. The crack growth volume strain shows a V-shaped trend with the increase of the seepage pressure. Taking 10 MPa confining pressure as an example, when the seepage pressure is 1, 3, and 5 MPa, the initial volume strains of cracks are 0.71×10^{-3}, 0.69×10^{-3}, and 0.41×10^{-3}, respectively, and the volume strains of crack propagation are -1.1×10^{-3}, -1.8×10^{-3}, and -0.6×10^{-3}, respectively.

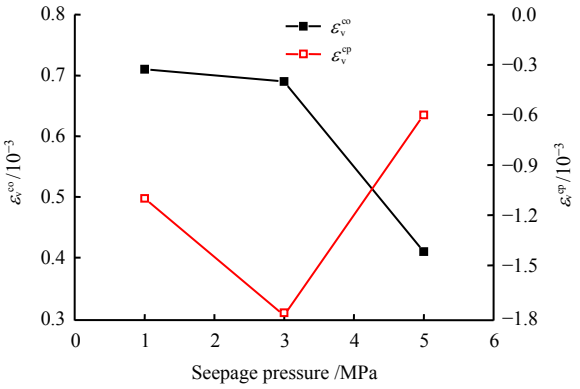

Fig. 6 The relation between crack volume strain and seepage pressure of sandstone under 10 MPa confinement

3.4 Crack growth rate

The crack growth rate has an important effect on the

deformation and damage process of sandstone [2,16–18]. According to the crack strain equations (Eq. (3) to Eq. (6)), the relation curves between crack strain and loading time during rock deformation are obtained, and the slope of any point on the curve is defined as the crack strain growth rate [2]:

$$V_i^{\mathrm{c}} = \frac{\mathrm{d}\varepsilon_i^{\mathrm{c}}}{\mathrm{d}t} \tag{7}$$

where V_i^{c} is crack strain growth rate; $\varepsilon_i^{\mathrm{c}}$ is crack strain, and i = 1, 3, denotes the first principal stress direction and the third principal stress direction, respectively; and t is the time.

In this study, the crack growth rate is calculated by taking the mean crack growth rate of three points. Figure 7 shows the relation between crack strain (corresponding to the damage stress and peak stress) and time under the conventional triaxial loading condition. Prior to the crack initiation stress, the crack axial strain, crack circumferential strain and crack volume strain fluctuate at low stress levels. At the stage of stable crack propagation, the tension crack gradually propagates along the crack tip and bifurcates to produce secondary cracks[13]. At the stage of unstable crack propagation, the crack strain continues to increase in all directions, then the internal cracks of the rock specimens present two types of cracks (i.e., tension and shear cracks), and macroscopic penetration cracks appear after reaching the peak stress level. After the peak stress, the tension cracking and shear slip lead to a sharp increase of the crack axial strain.

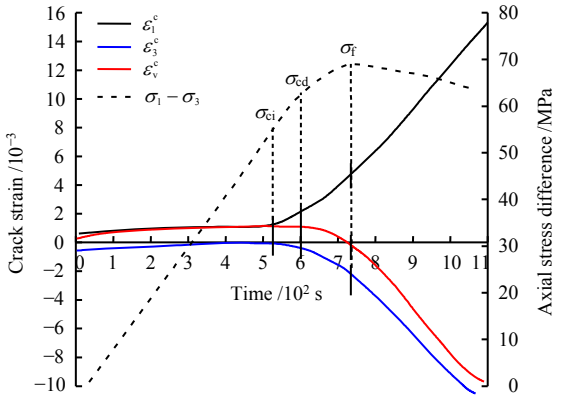

Fig. 7 The relation between crack strain and time of sandstone under 10 MPa confinement

Figure 8 shows the relation between confining pressure and crack growth rate corresponding to characteristic stress levels under conventional triaxial conditions. For the location of crack initiation stress, damage stress and peak stress, the strain growth rates follow the order: the crack axial strain > the crack circumferential strain > the crack volume strain. The strain growth rate corresponding to the characteristic stress level decreases with the increase of the confining pressure.

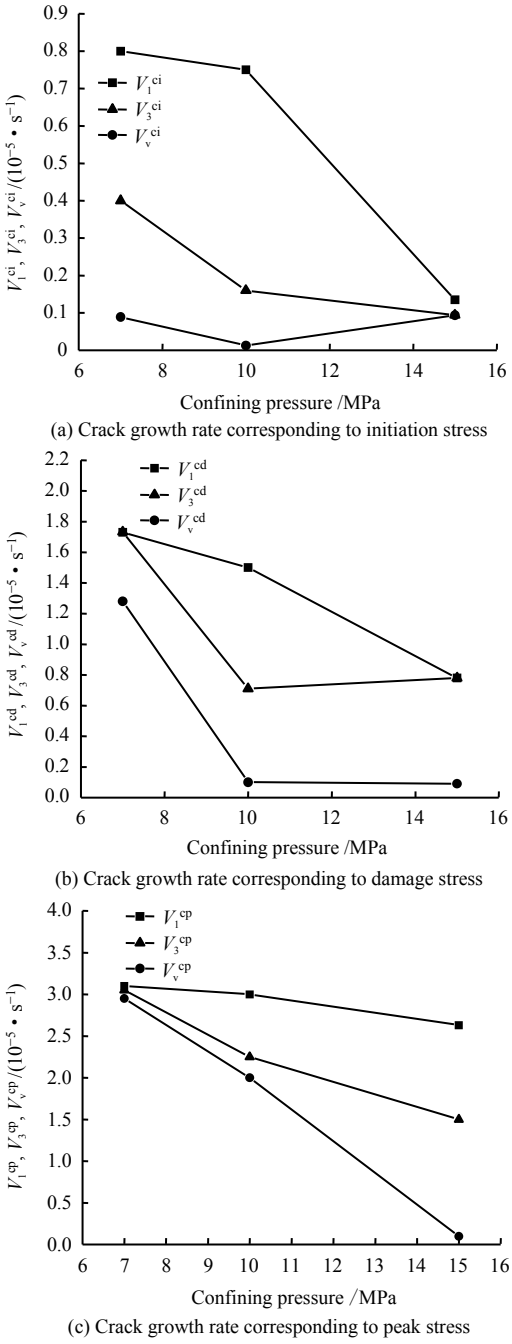

Fig. 8 The relation between crack growth rate and confining pressure corresponding to characteristic stress levels under conventional triaxial loading condition

When the elastic stage transits to the stable crack expansion stage, the new cracks initiate, and the crack volume strain growth rate is the minimum value during the loading process. As shown in Fig. 8(c), under the confining pressure of 7 MPa, the crack axial strain growth rate V_1^{cp}, crack circumferential strain growth rate V_3^{cp}, and crack volume growth rate $V_{\mathrm{v}}^{\mathrm{cp}}$ corresponding to the peak stress are 3.1×10^{-5}, 3.05×10^{-5}, 2.95×10^{-5}/s, respectively. When the confining pressure comes to 10 MPa, the crack growth rates corresponding to peak stress are 3.00×10^{-5}、2.25×10^{-5}、2.00×10^{-5}/s, respectively. In addition, the crack growth rates at different directions corresponding to peak stress

are 2.63×10^{-5}、1.50×10^{-5}、0.1×10^{-5}/s with a 15 MPa confining pressure, respectively. As the confinement increases from 7 MPa to 15 MPa, the decreasing extent in the crack volume strain growth rate reaches 2.85×10^{-5}/s corresponding to the peak stress, which is larger than the decreasing extent in the crack axial strain growth rate of 0.47×10^{-5}/s and the decreasing extent in the crack circumferential strain growth rate of 1.55×10^{-5}/s. This indicates that the crack volume strain growth rate is affected largely by the confining pressure corresponding to the peak stress of the rock under conventional triaxial conditions.

The crack strain growth rate corresponding to the peak stress is greater than that corresponding to the damage stress. Taking the test of 10 MPa confining pressure as an example (Fig. 8(b)), the crack axial strain growth rate, the crack circumferential strain growth rate, and the crack volume strain growth rate are 1.5×10^{-5}, 0.71×10^{-5}, and 0.1×10^{-5}/s corresponding to the damage stress level, respectively, which are smaller than the crack strain growth rate corresponding to the peak stress.

Figure 9 shows the relation between the crack strain and time under different seepage pressures with 10 MPa confining pressure. When compared with the conventional triaxial loading path, the time of sandstone deformation and damage process significantly decreases under seepage pressure, and the crack strain growth of peak stress is higher, which indicates that the seepage pressure can accelerate the crack expansion and lead to the earlier rock crack coalescence time.

Figure10 shows the relation between the crack growth rate and seepage pressure corresponding to the characteristics stress levels of the sandstone under different seepage pressures with the confining pressure of 10 MPa. When the seepage pressure increases, the crack strain growth rate corresponding to the initiation stress level increases firstly and then decreases. The growth rates of crack axial strain and circumferential strain corresponding to the damage stress and the peak stress levels increase. Among them, as the seepage pressure increases from 1 MPa to 5 MPa, the growth rate increments of the crack axial strain and circumferential strain corresponding to the damage stress are 0.5×10^{-5} and 0.72×10^{-5}/s, respectively. The growth rate increments of crack axial strain and crack circumferential strain corresponding to the peak stress are 1.40×10^{-5} and 0.90×10^{-5}/s, respectively. Under the confining pressure of 10 MPa and seepage pressure of 1 MPa, the growth rate increments of crack axial, circumferential and volume corresponding to the location of damage stress and peak stress are 0.7×10^{-5}, 0.57×10^{-5} and 0.37×10^{-5}/s, respectively. The axial crack growth rate is the most variable growth rate in the analysis.

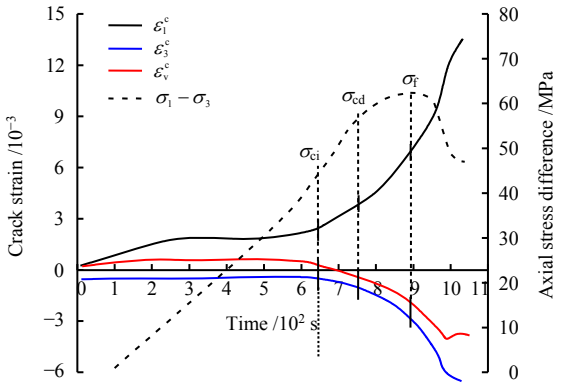

Fig. 9 The relation between the crack strain and time under the seepage pressure of 3 MPa and the confining pressure of 10 MPa

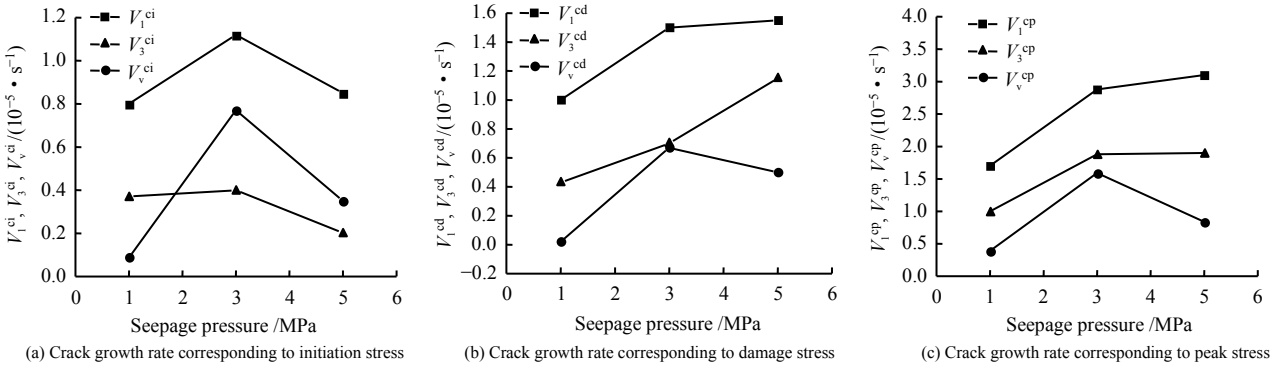

(a) Crack growth rate corresponding to initiation stress (b) Crack growth rate corresponding to damage stress (c) Crack growth rate corresponding to peak stress

Fig. 10 The relations between the crack growth rate and seepage pressure corresponding to the characteristics stress levels of sandstone under different seepage pressures with 10 MPa confinement

Figure 11 shows the statistics of crack strain growth rate corresponding to the characteristic stress levels of the sandstone. The crack strain growth rates of sandstone range from 0.1×10^{-5} to 3×10^{-5}/s. Compared with the tests of the seepage pressure of 3MPa and 5 MPa and the conventional triaxial test, the crack strain growth rate corresponding to the characteristic stress is the smallest when the seepage pressure is 1 MPa. Under the conventional triaxial with seepage pressures of 3 MPa and 5 MPa, the crack strain growth rates corresponding to the characteristic stress levels show a similar trend. Considering the test data, there is little effect of the seepage pressure on the crack strain growth rate in sandstone.

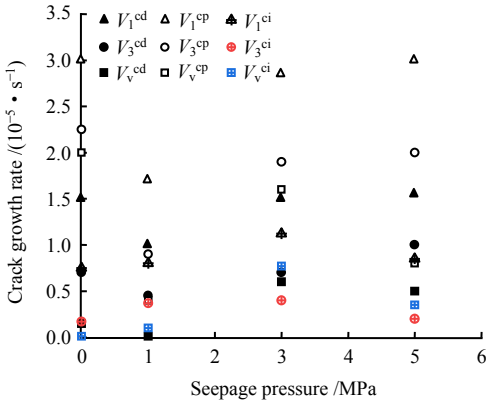

Fig. 11 The characteristics stresses corresponding to the crack strain growth rate under different seepage pressures

4 Conclusions

(1) As the confining pressure increases, the growth rates of the crack axial strain, circumferential strain and volumetric strain that corresponds to the crack initiation stress, damage stress and peak stress, respectively, decrease gradually. The crack volume strain growth rate corresponding to the peak stress is affected most by the confining pressure.

(2) The brittleness index increases as the seepage pressure increases, while the crack initiation stress, damage stress, peak stress and the crack initial volume strain decrease. In addition, the volumetric strain of crack growth shows a V-shaped trend, which decreases first and then increases afterwards. The crack growth rate increases that corresponding to the damage stress and the peak stress levels.

(3) As the effective confining pressure increases, the characteristic stress level increases and the corresponding crack strain growth rate also increases. Under the action of seepage pressure, the ratios of crack initiation stress, and crack damage stress to the peak stress ranges from 0.63 to 0.79, and 0.81 to 0.94, respectively. The smaller the confining pressure and the greater the seepage pressure, the greater the characteristic stress levels and the corresponding crack growth rate.

References

[1] BIOT M A. General theory of three-dimensional consolidation[J]. Journal of Applied Physics, 1941, 12(2): 155−164.

[2] CHEN Yan. Study on deformation failure behaviors and nonlinear models for rocks under the influence of mining disturbance[D]. Beijing: China University of Mining & Technology, 2018.

[3] YU Jin, LI Hong, CHEN Xu, et al. Triaxial experimental study of associated permeability-deformation of sandstone under hydro-mechanical coupling[J]. Chinese Journal of Rock Mechanics and Engineering, 2013, 32(6): 1203−1213.

[4] ZHAO Kai, WANG Huan-ling, XU Wei-ya, et al. Experimental study on seepage characteristics of rock-like materials with consecutive and filling fractures[J]. Chinese Journal of Geotechnical Engineering, 2017, 39(6): 1130−1136.

[5] PENG Su-ping, MENG Zhao-ping, WANG Hu, et al. Testing study on pore ratio and permeability of sandstone under different confining pressures[J]. Chinese Journal of Rock Mechanics and Engineering, 2003, 22(5): 742−746.

[6] HU Da-wei, ZHOU Hui, XIE Shou-yi, et al. Study of Biot coefficients of marble during plastic deformation phase[J]. Rock and Soil Mechanics, 2009, 30(12): 3727−3732.

[7] PARK H D. Fluid permeability of sedimentary rocks in a complete stress-strain process[J]. Engineering Geology, 2002, 63(3/4): 291−300.

[8] LI S P, WU D X, XIE W H, et al. Effect of confining pressure, pore pressure and specimen dimension on permeability of Yin Zhuang sandstone[J]. International Journal of Rock Mechanics and Mining Sciences, 1997, 34(3-4): 175.e1-175.e11.

[9] BIENIAWSKI Z T. Mechanism of brittle fracture of rock[J]. International Journal of Rock Mechanics and Mining Sciences & Mechanics Abstracts, 1967, 4(4): 395−430.

[10] MARTIN C D. The strength of massive Lac du bonnet granite around underground openings[D]. Manitoba, Canada: University of Manitoba, 1993.

[11] WANG Wei, ZHENG Zhi, WANG Ru-bin, et al. Experimental study on permeability characteristics of granite gneiss under different stress paths[J]. Chinese Journal of Rock Mechanics and Engineering, 2016, 35(2): 260−267.

[12] ZHOU Z H, CAO P, YE Z Y. Crack propagation mechanism of compression-shear rock under static dynamic loading and seepage water pressure[J]. Journal of Central South University, 2014, 21(4): 1565−1570.

[13] CAO Jia-xing, ZHU Zhen-de, TIAN Yuan, et al. The experimental study of propagation progress of 3D crack sets under hydraulic pressure[J]. Science Technology and Engineering, 2017, 17(4): 92−98.

[14] WANG C, ZHANG Q Y. Study of the crack propagation model under seepage–stress coupling based on XFEM[J]. Geotechnical & Geological Engineering, 2017(6): 1−12.

[15] China Electricity Council. GB/T 50266—2013 Standard for test methods of engineering rock mass[S]. Beijing: China Planning Press, 2013.

[16] ZHANG L M, CONG Y, MENG F Z, et al. Energy evolution analysis and failure criteria for rock under different stress paths[J]. Acta Geotechnia, 2021, 16(2): 569−580.

[17] LIU Jie, ZHANG Li-ming, CONG Yu, et al. Study of Biot coefficients of marble during plastic deformation phase[J]. Rock and Soil Mechanics, 2021, 42(8): 2069−2077.

[18] ZHANG Q B, ZHAO J. Effect of loading rate on fracture toughness and failure micro mechanisms in marble[J]. Engineering Fracture Mechanics, 2013, 102(2): 288−309.